

## GROWTH OF SiC FILMS BY THE METHOD OF SUBSTITUTION OF ATOMS ON POROUS Si (100) AND (111) SUBSTRATES

V.V. Kidalov<sup>1</sup>, S.A. Kukushkin<sup>2,3\*</sup>, A.V. Osipov<sup>2,3</sup>, A.V. Redkov<sup>3</sup>, A.S. Grashchenko<sup>2</sup>,  
I.P. Soshnikov<sup>4,5</sup>, M.E. Boiko<sup>5</sup>, M.D. Sharkov<sup>5</sup>, A.F. Dyadenchuk<sup>1</sup>

<sup>1</sup>Berdiansk State Pedagogical University, 4, Shmidta St., Berdyansk, 71100, Ukraine

<sup>2</sup>Institute of Problems of Mechanical Engineering, Bolshoj pr. 61, Vas. Ostrov, St. Petersburg, 199178, Russia

<sup>3</sup>ITMO University, Kronversky pr. 49, St. Petersburg, 197101, Russia

<sup>4</sup>Saint Petersburg National Research Academic University, Khlopina 8/3, St. Petersburg, 194021, Russia

<sup>5</sup>Ioffe Institute, Politekhnikeskaya 26, St. Petersburg 194021, Russia

\*e-mail: sergey.a.kukushkin@gmail.com

**Abstract.** The mechanisms of growth of silicon carbide (SiC) films by the method of substitution of atoms on macro- and mesoporous silicon substrates (Si) of p- and n-type conduction are investigated. Significant dependence of the rate and the mechanism of nucleation of SiC layers on Si on the type of Si doping and its crystallographic orientation is experimentally found. Comparison of the experimental data with the theoretical results obtained earlier is performed. It is shown that the presence of the system of pores on the surface allows one to significantly increase the thickness of silicon transformed into SiC during the process of synthesis by the method of substitution of atoms, which was equal to 115 microns in our experiments. The obtained samples are studied by methods of scanning electron microscopy, micro-Raman spectroscopy, and X-ray diffraction analysis. Numerical simulation of the distribution of elastic stresses caused by the difference in thermal expansion coefficients (TEC) in the heterostructures of GaN/SiC/porous Si/Si is conducted. It is revealed that the presence of pores in the near-surface layers of Si leads to considerable relaxation of elastic stresses in GaN films caused by differences in the TEC between GaN and Si.

**Keywords:** silicon carbide; epitaxial films SiC on Si; epitaxy; gallium nitride films; aluminum nitride films; thin films growth; porous silicon substrate.

### 1. Introduction

One of the topical directions of thin-film technology advancement is the development of methods of high-quality (low defect density) film growth of wide-bandgap semiconductors such as aluminum nitride (AlN), gallium nitride (GaN), silicon carbide (SiC), and gallium oxide (Ga<sub>2</sub>O<sub>3</sub>). The major difficulty arising during epitaxy of such materials is that their own substrates are either absent or expensive [1]. In this regard the search of the foreign substrates that allow growing of GaN and AlN thin films of quality that is necessary for instrument structures continues. Sapphire, silicon carbide (SiC) and silicon (Si) are the most suitable for this purpose [1]. At present, the last two substances are gradually displacing sapphire. Each of these materials has its own advantages and disadvantages [1]. When commercially available and easy-to-grow silicon is being used, a number of difficulties arise that are connected with the difference in the thermal expansion coefficients (TEC) and in lattice parameters, which negatively affect structural perfection of the growing GaN films and cause the emergence of

high-density of dislocations. Monocrystalline SiC substrates are almost devoid of these shortcomings, but they are extremely expensive to produce [1]. In a series of works generalized in reviews [2, 3], the method of chemical substitution of atoms was proposed, allowing one to successfully combine the advantages of both silicon carbide and silicon and to obtain thin monocrystalline SiC films on Si substrates in relatively low-temperature processes (1200-1350 °C) which do not demand high energy consumption. The distinctive feature of this method is that the silicon carbide film is formed directly in the near-surface volume of the substrate and of its material – silicon by means of the substitution of a portion of Si atoms by C as a result of chemical reaction [2-4]:



Due to the fact that volumes of crystalline cells of silicon carbide and silicon differ almost twice ( $160.1 \text{ \AA}^3$  Si and  $81.5 \text{ \AA}^3$  SiC [2, 3]), during the transformation of silicon into SiC there inevitably occurs volume relaxation that leads to the formation of a porous structure under the SiC film surface [2-4]. Such a structure mechanically «detaches» silicon carbide film from the substrate, reduces contacting area, and allows one to efficiently decrease the elastic stresses arising owing to the difference in the TEC and lattice parameters during the growth of subsequent layers on SiC/Si substrate. A detailed description of a porous structure under a SiC layer and its influence on further growth is given in the reviews [2, 3] and works [4-10]. Up to now, high quality thin GaN and AlN films [11, 12] and those from some other materials [13] have already been grown on such substrates by various methods: hydride vapour phase epitaxy (HVPE) [12], molecular beam epitaxy (MBE) [14], metalorganic chemical vapour deposition (MOCVD) [15], etc. The research on the other porous substrates was conducted which also showed the effectiveness of this approach. Thus in the works [16, 17] GaN films of cubic modification on porous substrates of gallium arsenide (GaAs) were obtained by the method of radical beam epitaxy. It was shown that a part of the elastic deformations arising in the heterostructure of GaN/porous GaAs/GaAs [18] relaxes just in a porous structure.

In this regard, further research on the process of formation of a porous structure in the SiC/Si system and its influence on the elastic stresses in the system seems to be relevant. It should be noted that despite its positive role in considerable stress relaxation, the pores in the SiC/Si structures obtained by the method of substitution of atoms are chaotically located and often have a random shape, which results in nonuniform stress field. In order to overcome these shortcomings, it is suggested in this paper to apply an artificial periodic system of deep pores on the surface of silicon before building-up a layer of SiC, which would allow solving a number of problems simultaneously. Firstly, such a system would allow one to significantly increase the thickness of the obtained SiC layer, as the depth of CO penetration into the substrate will be determined only by the depth of the pores. Secondly, the existence of a «skeleton» from the previously formed system of pores will allow one to eliminate the disorder, and the pores that are formed in the process of transformation of Si into SiC will «inherit» the given structure. By regulating the period and geometrical sizes of the «skeleton» pores, it is possible to optimize the distribution of elastic stresses in the system. Thirdly, the existence of a periodic porous structure on the surface of SiC/Si allows using this substrate for pendeo-epitaxy of various semiconductors. Thus, in the work [19] authors carried out AlN pendeo-epitaxy on the surface of SiC/Si substrate, on which a grid of wells of the size of about 200 nanometers was formed by the method of electron lithography. The existence of this grid allowed them to reduce mechanical stress and to increase the quality of AlN film on SiC/Si substrate.

The purpose of this work is to investigate the processes of formation of silicon carbide by the method of topochemical substitution of atoms [2-6] on silicon (100) and (111) substrates with the previously formed system of pores of macro- and meso-sizes. The first

part of this paper describes experimental methods of formation of pore pattern in silicon and the growth of SiC/porous Si/Si structures. The second part contains the results and discussion of the study of the obtained samples via the following methods: Raman spectroscopy, X-ray diffractometry, and scanning electron microscopy. The X-ray diffraction measurements were performed using DRON-UM-1.0 facility (Cu K $\alpha$ 1 radiation, a wavelength  $\lambda=1.5405$  Å), Raman spectra were obtained by means of a confocal Raman microscope Witec Alpha 300R, and the structure of SiC/Si interface and the structure of SiC layers were studied using scanning electron microscope Zeiss Supra 25. The results of numerical simulation by the finite element method of the process of substrate cooling with such a porous system are reported in the third part of the paper, and it is shown that mechanical stresses arising during the film cooling due to the difference in TEC are being significantly reduced.

## 2. Materials and Methods

### Synthesis conditions of SiC layers on macro- and mesoporous Si (100) and (111).

The following substrates were used for SiC growth:

- macroporous silicon Si (100) of *n*-type, the pore diameter is  $\sim 500$  nm, the average depth of the porous layer is  $\sim 150$   $\mu\text{m}$ , and the distance between the pore centers is  $\sim 1.4$   $\mu\text{m}$  (Fig. 1a,b).
- mesoporous silicon Si (100) and Si (111) of *p*-type, the pore diameter is about 17 nm, the depth of the porous layer is  $\sim 240$  nm (Fig. 1c,d). The pores for both macro- and mesoporous Si (100) are perpendicular to the Si surface and have the shape close to a cylindrical one. The pores in Si (111) are located at certain angle to the surface.

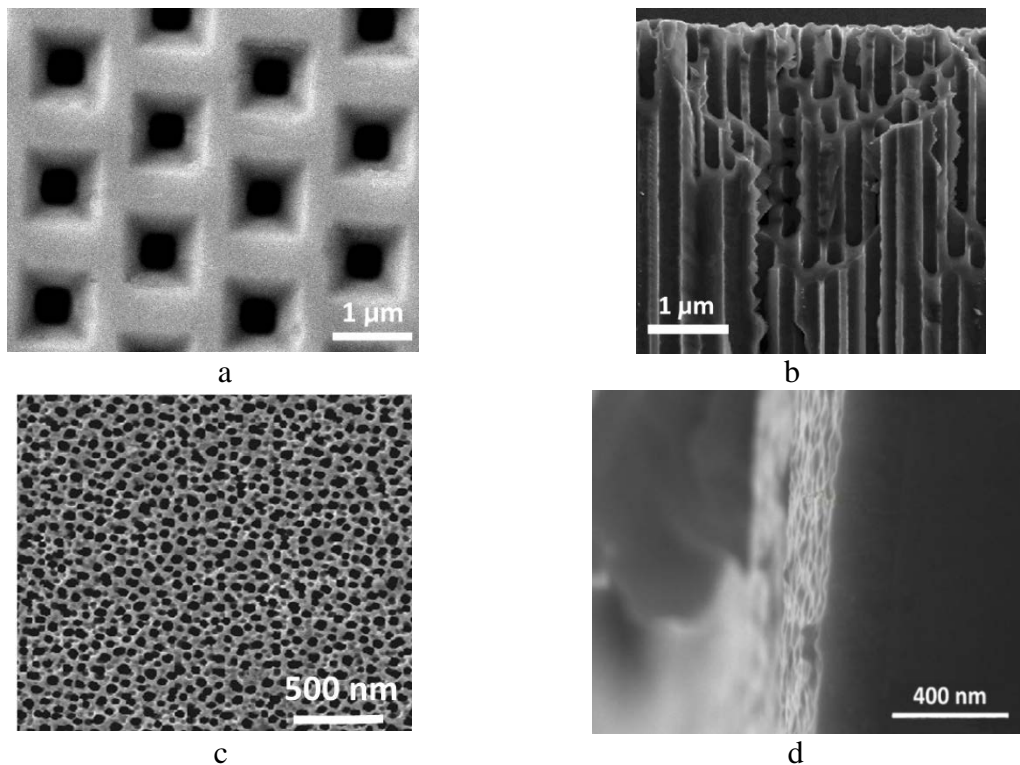


**Fig. 1.** SEM images of the surface and cross-sections of Si (100) samples with the ensemble of macropores (a, b) and mesopores (c, d).

A standard technology has been used to apply an ordered micro-porous structure [16-18]. We note that the etching rate in the [111] direction is minimal and an order of magnitude less than the etching rate in the [100] direction. Figure 1 shows scanning electron microscopy

(SEM) micrographs of the surface and lateral sections of the profiled Si (100) with the ensemble of macro - (a, b) and mesopores (c, d).

Silicon carbide layers were grown on the samples of macro- and mesoporous Si by the method of substitution of atoms [2-6]. For this purpose, the samples were annealed in the atmosphere of gas mixture of carbon monoxide (CO) and silane ( $\text{SiH}_4$ ). A detailed description of the process of SiC growth and the experimental installation diagram are presented in the review [3]. The synthesis parameters are presented in Table 1. One of Si(111) samples was grown under different conditions. These conditions are summarized in Table 2.

Table 1. Conditions of the synthesis of the samples Si(100) and Si(111), profiled by macro- and mesopores.

Parameter	
Growth temperature, °C	1290
Growth time, min	20
Pressure of the gas mixture ( $\text{CO}+\text{SiH}_4$ ), Pa	53
CO gas flow, sccm	12
$\text{SiH}_4$ gas flow, sccm	3,5

Table 2. Conditions of the synthesis of SiC layer on the second mesoporous Si(111) sample.

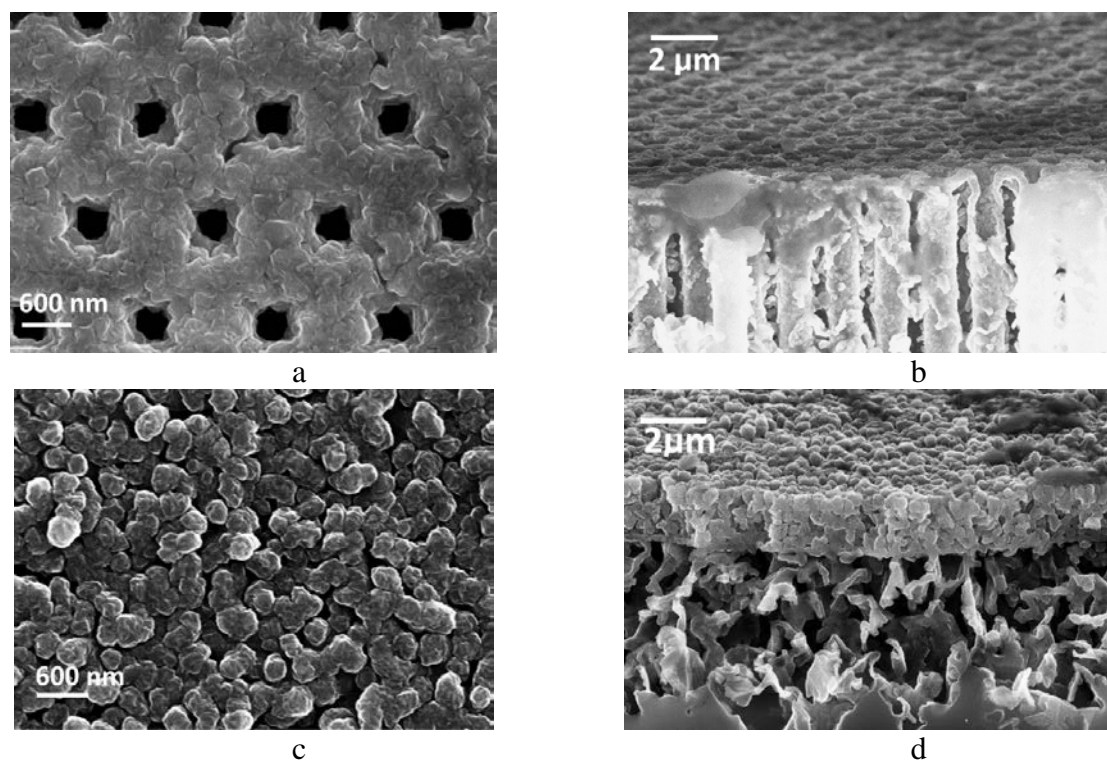
Parameter	
Growth temperature, °C	1290
Growth time, min	20
Pressure of the gas mixture ( $\text{CO}+\text{SiH}_4$ ), Pa	133
CO gas flow, sccm	14
$\text{SiH}_4$ gas flow, sccm	3,5

After the synthesis the samples were investigated by SEM, confocal Raman spectroscopy and XRD.

### 3. Results

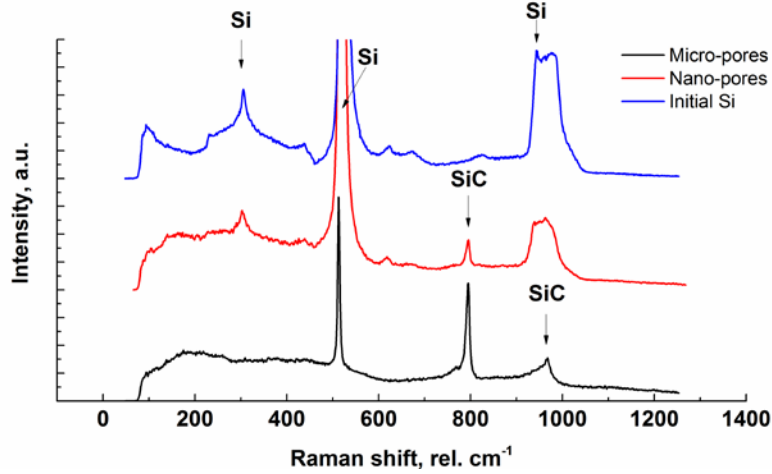
**SiC layers on macro- and mesoporous Si (100) substrates.** The SEM images of the surface and cross-sections of the SiC/porous Si/Si heterostructure samples demonstrate a significant change in the surface morphology after the synthesis. Thus, on the surface of both samples a structure of small crystallites from about tens to one hundred nanometers can be observed. A sample with macropores retained the original structure in the form of the grid. The pore diameter on the sample with macropores (Fig. 2a), according to the SEM, decreased almost 2 times from the initial 500 nm to 250-300 nm. On the cross-section of this sample (Fig. 2b), one can see that the space among the pores that was previously occupied by silicon has become empty, and the walls surrounding the pores have the thickness of about 150 nanometers. Thus, taking into account the reduction in the pore diameter, we can estimate that the volume which became vacant from the silicon is close to the volume occupied by the silicon carbide after the growth process. This well agrees with the fact that the volume of the crystalline cell of a cubic polytype of SiC ( $81.5 \text{ \AA}^3$ ) is about half the size of a silicon cell ( $160.1 \text{ \AA}^3$ ) [1, 2]. The depth, at which changes in the structure of the substance are observed is

about 115  $\mu\text{m}$  according to the SEM measurements. It should be noted that the original pore structure was not preserved on the sample with mesopores (Fig. 2c) and its surface is uniformly covered with crystallites. The depth of the carbide formation is about several microns. The SEM image of the cross-section of this sample (Fig. 2d) shows that the film is practically «hanging» over the Si substrate and the volume of the hollow spaces under it greatly exceeds the usually observed one after growth by the method of substitution of atoms [2-6].



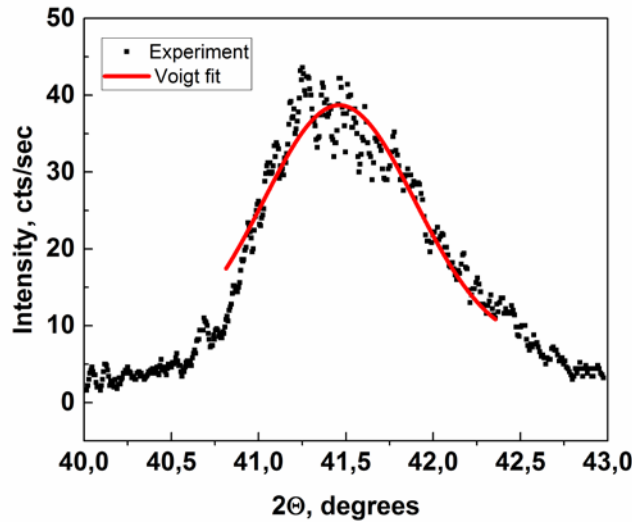
**Fig. 2.** SEM images of the surface and cross-section of the SiC layers formed on the surface of macroporous (a, b) and mesoporous (c, d) silicon.

Figure 3 shows the Raman spectra of the samples before and after the treatment in the atmosphere of gases mixture of carbon monoxide (CO) and silane ( $\text{SiH}_4$ ). The samples spectra after the treatment demonstrate the presence of 3C-SiC cubic polytype lines in the region of  $794\text{ cm}^{-1}$  and  $965\text{ cm}^{-1}$  [20] as well as silicon lines of  $521\text{ cm}^{-1}$  [20]. The lines corresponding to hexagonal polytypes of SiC were not observed [2]. It should be noted that the intensity of the SiC lines is much higher on the sample with macropores. Apparently, it is caused by a thicker film.



**Fig. 3.** Raman spectrum of the original silicon (upper) and SiC/Si structures with meso- (medium) and macropores (lower).

The X-ray diffraction analysis of the samples also showed unambiguous presence of only the cubic phase of silicon carbide by the presence of reflexes from (002), (113), (115), and (224) planes, besides the latter ones repeated with an azimuthal rotation of the sample every 90° around the [001] axis. Thus, the epitaxial growth of 3C-SiC films was oriented along the [001] direction perpendicular to the physical plane of the substrate, i.e. it coincided with the [001] axis of the silicon substrate. Fig. 4 shows the shape of the (002) reflex of silicon carbide.



**Fig. 4.** X-ray diffraction pattern of the (002) peak from 3C-SiC films grown on mesoporous Si (100) substrates.

The study of the shape of (002) reflex (Fig. 4) made it possible to estimate the sizes of the cubic SiC crystallites. For this purpose, the Selyakov-Scherer model was used [21] that links crystallite  $L$  size in the direction corresponding to the given reflex, and the full width of the reflex at half maximum (FWHM).

$$L = \frac{K\lambda}{\beta \cos \theta}, \quad (2)$$

where  $\lambda$  is a wavelength;  $\beta$  – reflection width at half-maximum in radians (FWHM along  $2\theta$ –scale);  $\theta$  – diffraction angle (Bragg angle);



$$K = \frac{6h^3}{\sqrt{h^2 + k^2 + l^2} (6h^2 - 2hk + kl - 2hl)}, \quad (3)$$

where  $h, k, l$  – Miller indices. It follows from the expression (3) that  $K=1$  for the (002) reflex. An estimation of the width of the (002) reflex in the Voigt approximation (solid line in Fig. 4) gives a value of about 1.1 degrees for  $\beta$ .

Hence, it follows from the Fig. 4 that the crystallite size in (001) direction, i.e. its thickness, is approximately 27.5 nm. This is a very reasonable value of the thickness of the crystallites.

One can see from the Fig. 2a that the SiC layer along (001) direction consists of disc-like "plates" lying on top of each other. An approximate estimation by a comparison with the scale bar in the figure shows that their thickness is definitely within the range of 20 – 60 nm. Thus, the obtained estimates of the sizes of cubic SiC particles agree with the assumption about the shape of the particles. However, it should be accounted that the broadening of the X-ray reflections is caused not only by the sizes of the grains (Selyakov-Scherer equation), but also by a microdeformation of the atomic lattice of the sample, as well as by instrumental factors. Therefore, the actual sizes of nanoclusters consisting of particle conglomerates can be much larger than the values calculated from the FWHM estimations in accordance with the Selyakov-Scherer model [21].

**SiC layers on mesoporous Si (111) substrates.** Figure 5 (a-d) shows SEM images of the SiC samples grown on mesoporous Si (111). For comparison, in Fig. 6 we provide typical [2-12] images of cross-sections of Si samples with a SiC layer grown by the method of substitution of atoms on monocrystalline Si (100) and (111) substrates.

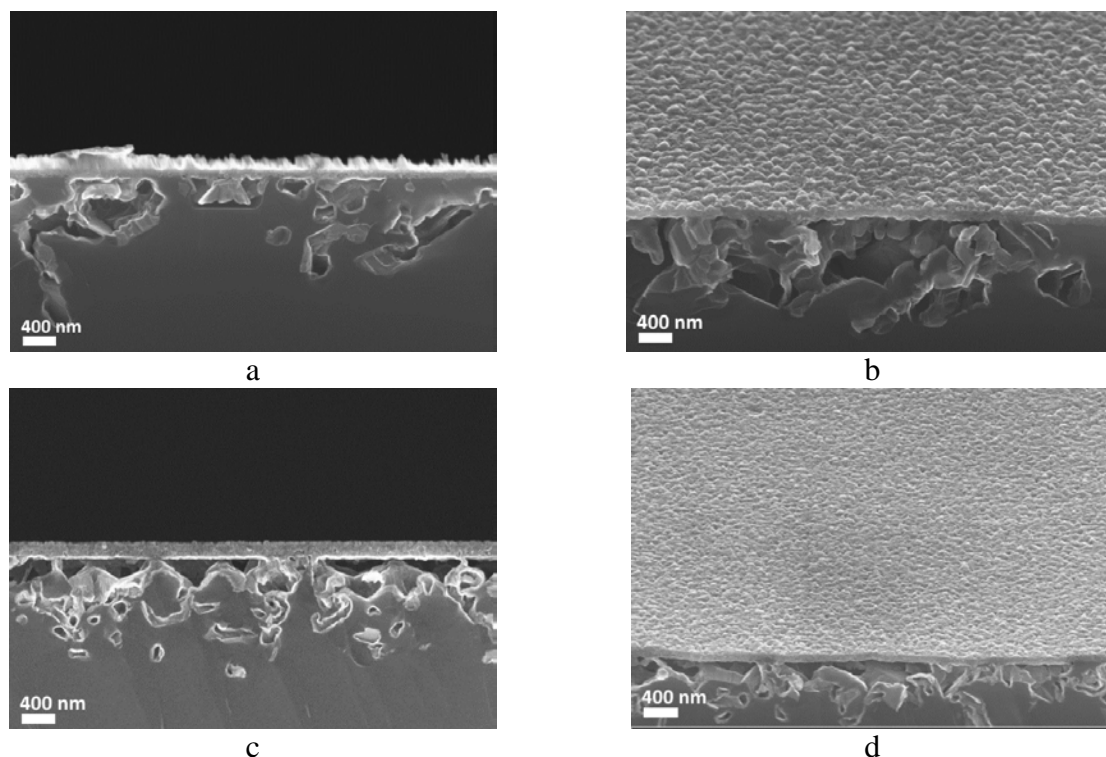


**Fig. 5.** SEM images of the cross-section (a, c) and surface (b, d) of the SiC layers synthesized on the Si (111) surface with a previously formed mesopore system at different CO gas pressures: (a, b) – CO pressure is  $PCO=53$  Pa; (c, d) – CO pressure is  $PCO=133$  Pa.

Comparing Fig. 5 (a-d) and Fig. 6 (b) one can see that the morphology structure of SiC surfaces grown on the monocrystalline and mesoporous Si (111) practically coincide. The SiC

surface grown at low CO pressure ( $P_{CO}=53$  Pa) in Fig. 5a,b is very rough, at a higher CO pressure ( $P_{CO}=133$  Pa) in Fig. 5c,d it is smooth. The effect of an almost complete peeling of the SiC film (Fig. 5) from the Si surface was quite interesting. This layer has only an insignificant contact with Si, which distinguishes it clearly from the SiC layer grown under the same conditions on monocrystalline Si [3]. This is a very important effect for the use of such structures as a buffer layer for further growth of epitaxial films of wide-bandgap semiconductors of various composition on their surface.

One could observe a totally different picture of SiC films growth on the mesoporous surfaces of Si (100) (Fig. 2c and Fig. 2d) and monocrystalline surface of Si, the typical SEM [2-12] image of which is shown in Fig. 6a. On the porous surface SiC layer consists of separate grains rotated in different directions while on the monocrystalline surface we can see almost a smooth interface between SiC and Si and a smooth surface of SiC. The SiC layer is polycrystalline on the surface of Si (100) covered with pores, whereas as shown in the works [2-7], an epitaxial layer of SiC grows on the surface of Si (100) that is free from the pores.

Depending on the CO pressure, the SiC layer grown on the Si (111) mesoporous surface can be either polycrystalline or epitaxial, according to the electron diffraction pattern data in Fig. 7. Indeed, the Fig. 7 shows the electron diffraction photographs taken from the surface of the SiC layers grown at the CO pressures  $P_{CO} = 53$  Pa (Fig. 7a) and  $P_{CO} = 133$  Pa (Fig. 7b), SEM images of which are shown in the Fig. 5, from which one can clearly see that SiC layers grown on the Si(111) surface profiled with pores can be both textured (Fig. 7a) and epitaxial (Fig. 7b).

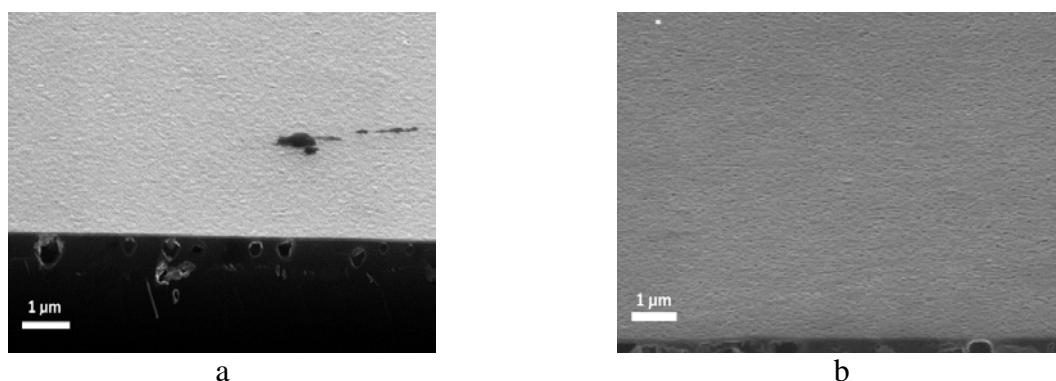


**Fig. 6.** Typical SEM images of the cross-section and surface of Si samples with a SiC layer grown by the method of substitution of atoms [2] on monocrystalline Si (100) (a) and (111) (b) substrates.

The Figures 7c and 7d show electron diffraction photographs taken from the surface of SiC layers grown under exactly the same conditions as the films whose electron diffraction patterns are shown in the Fig. 7a and Fig. 7b and on the same silicon but not profiled with the pores. One can clearly see that the electron diffraction pattern in the Fig. 7c corresponds to the epitaxial single-crystal layer. The SiC layer, electron diffraction pattern of which is shown in the Fig. 7d, contains a certain number of twins, i.e. it is somewhat worse in quality than the layer grown at the CO pressure  $P_{CO} = 53$  Pa. This fact completely corresponds to the theoretical conclusion proved in the review [2] that the higher the density of dislocations or other linear defects in Si, in particular, pores created artificially, the greater the CO pressure should be in the reactor for the synthesis of epitaxial films. This is due to the fact that with increasing CO pressure, the rate of formation of a continuous SiC layer increases, which inhibits the access of CO gas into the deep of the Si substrate and does not result in its etching under the SiC layer.



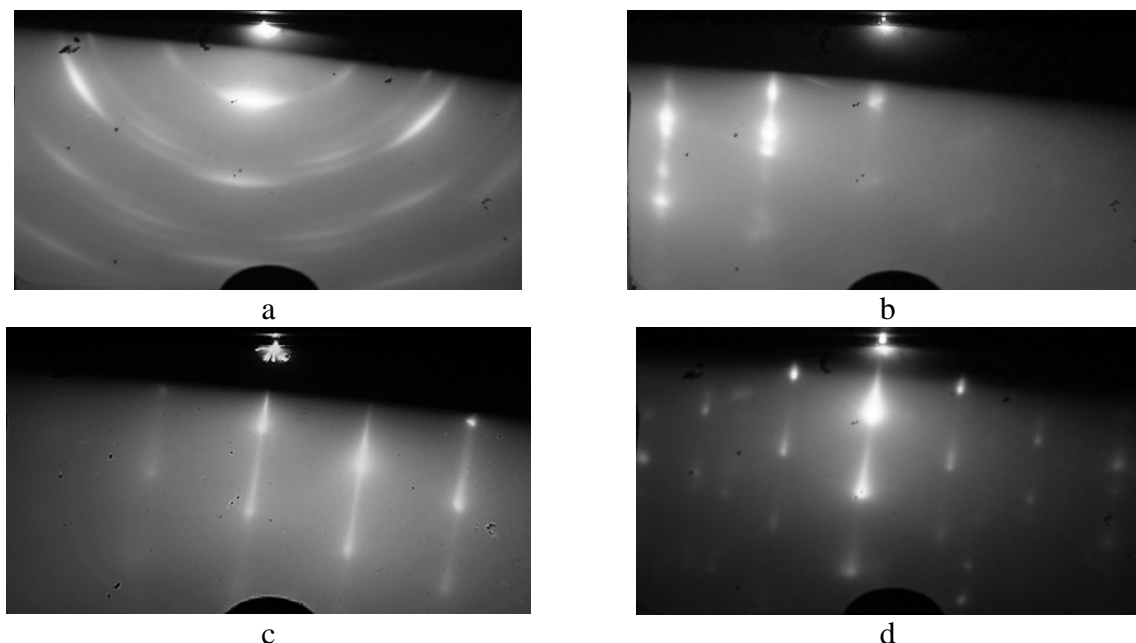


**Fig. 7.** Electron diffraction patterns of the surface of SiC on mesoporous (a, b) and flat (c,d) Si(111) synthesized under different CO gas pressures: (a, c) – the CO pressure is  $P_{CO}=53$  Pa (see Table 1); (b, d) – the CO pressure is  $P_{CO}=133$  Pa (see Table 2).

**The mechanisms of SiC growth on a porous surface of Si (100) and Si (111) of n- and p-type of conduction.** Thus, the experiment showed that the existence of pores in Si ensures more intensive penetration of CO gas deeper into the substrate and, as a result, to more "vigorous" rate of chemical reaction of CO with silicon. In the presence of pores in a substrate, the reaction of the transformation of Si into SiC affects a considerably larger volume of Si substrate than the reaction of CO with a flat silicon since CO gas penetrates into silicon volume through the pores.

The mechanism of formation of SiC layer on a porous Si surface is as follows. According to the theoretical provisions that are confirmed by numerous experiments [2, 3, 5-7], the reaction (1) occurs in several stages. In the beginning, the couples of point defects are being formed in a crystal lattice, namely a silicon vacancy and a carbon atom in an interstitial position. Such couples of defects are called dilatation dipoles by analogy with electric dipoles [2, 5-7]. These defects elastically interact among themselves. This interaction plays an important role in formation of SiC film in the volume of Si crystal [2, 5-7]. In particular, the most favorable arrangement of this couple of point dilatation defects is direction [111] [2, 5-7]. In this case, the total elastic energy of the system decreases dramatically, and the elastic stresses are being almost completely relaxed. Thus, according to the model of drift epitaxy which was developed in the work [6], the molecules of CO penetrate deep into a Si crystal not due to the routine Brownian motion but, first, due to the drift of CO molecules along the channels in a Si crystal saturated with dilatation dipoles of "C+V<sub>Si</sub>" (where V<sub>Si</sub> is a Si vacancy), and then along the SiC channels due to the pressure difference of CO outside of and inside the crystal. The growth of a film according to this model stops because the reaction product "clogs" the channels of the crystal, reducing their hydraulic diameter. The process reminds the formation of cholesterol plaques in blood vessels. That is an essential difference between this model and the diffusional one where increase in the thickness of a film continues infinitely as  $\sqrt{t}$ . In the work [6], for the first time, experiments were carried out to measure the maximum thickness of the film on Si(111) and Si(100) and its dependence on the pressure, and it was shown that there is a pressure corresponding to the maximum film thickness. With a further increase of the pressure, the

thickness of the film decreases, whereas it should increase in case of ordinary diffusion growth, since the diffusion intensifies in this case.

In a short time of growth, [6], the drift law of the growth of a film coincides with the diffusion one. As shown in [6], if the walls of a channel in Si crystal prevent reagent gas penetration and weakly interact with it, then the reagent can penetrate deeper in a short time. In this case, the velocity of the reagent is constant, determined by the Bernoulli equation for the flow of a viscous gas flow and according to it the order of magnitude is  $0.1\text{--}1\text{ }\mu\text{m/min}$ . In this case, in addition to the film, there grow the conglomerates of ribbon crystals that partially fill the voids in the initial substrates.

Similar conglomerates of crystals are also well observed during the growth of SiC on porous Si. Thus, for example, in Fig. 2d, one can see an ensemble of conglomerates, which is between the upper SiC layer and the main Si substrate. The voids are formed because the volume of a new phase is half of an old one. If the reaction product gas has not gone outside and partially remained in any area of a crystal, then considerable elastic stresses caused by the pressure of this gas exist in this area. When the gas escapes outside, funnels appear on the film surface with a diameter of about  $10\text{ }\mu\text{m}$  similar to volcanoes [2]. With the increase in pressure when the reaction product "clogs" the channels, such funnels on the surface disappear [2]. This process, which was theoretically predicted in the work [2], can be well observed during the growth of SiC on Si covered with the ensemble of periodic macropores when comparing Fig. 1a,b with Fig. 2a,b. In Figures 1a and 2a, one can see that after the synthesis the pores, which initially had the size of about  $500\text{ nm}$ , narrowed to  $250\text{--}300\text{ nm}$ . At the same time, their initial shape close to square became "fuzzy" and more similar to an irregular-shaped circle. Moreover, one can see very well in Fig. 2a that the SiC film consists of a great number of layers or crystallites having a flat shape. As we showed above, by means of an X-ray analysis, the thickness of these crystallites is about  $27.5\text{ nm}$ . These crystallites (flat crystalline scales) remind camera lens shutters which, when closed, move along each other, narrowing its hole. Thus, in this case, during the process of transformation of Si channels into SiC channels, they are being partially closed thereby reducing the access of CO to the internal Si areas. On a mesoporous substrate the pores (Fig. 2c, d) are completely closed. It should be noted that, according to the recently developed theory [22], the rate of the upper SiC crust formation (it especially refers to silicon (100)), depends heavily on the type and the level of its doping. The whole point of it is that during SiC growth by the atom substitution method [2], irrespective of an initial crystallographic Si plane, on which SiC was synthesized, plane (111) is obligatory being formed as one of the planes. This effect is due to the fact that for a cubic crystal the most favorable arrangement of dilatation dipole is perpendicular to plane (111). As a result, if the synthesis of SiC is carried out on the crystal face of (100) Si, then it does not turn into a crystal face of (100) SiC, but turns into the crystal face consisting of a great number of the facets that remind saw-toothed structures, the side faces of which are covered with planes (111), (110) and (210). The lower is pressure of CO, the more intensively the process of transformation of (100) grain into facets (111) goes, and vice versa the higher CO pressure lead to formation of more morphologically smooth SiC closer in form and crystallography to crystal face (100).

As shown in the work [24], in the silicon of *n*-type of conduction the lifetime of elastic dipoles is considerably less than their lifetime in the silicon of *p*-type of conduction. Therefore, the channels will be "closed" quickly in Si of *n*-type of conduction. As a result, the layers of SiC will have a sandwich structure. In fact, this phenomenon is observed during the SiC growth on the pore-covered surface of Si (100) of *n*-type of conduction. Only a very large diameter of pores does not allow the pores to be closed completely.

The other situation arises on the surface of Si (100) of *p*-type of conduction. The lifetime of elastic dipoles on this type of silicon much longer than on Si (100) of *n*-type of

conduction. As a result, CO gas penetrates deeply into Si through silicon vacancies. Instead of SiC layers, the planes (111) are formed on all the way of CO movement. As far as Si became rather friable after etching, the formation of multidirectional planes leads to mass peeling of the SiC nuclei from Si matrix. At the same time the SiC nuclei are being covered with an array of facets (111) and take an irregular spherical shape. When the pores are small, they fill them almost completely. It is what we observe on the example of SiC growth on the mesoporous Si surface (100) (Fig. 2c,d). Under a layer of a friable SiC crust, the whole volume of Si is covered with conglomerates of ribbon crystals of SiC which are the remnants of the former channels on which the molecules of CO moved.

On the surface of Si (111), the formation process of SiC depends to a lesser extent on the type and level of doping. Therefore, in case of SiC growth with a low pressure of CO, the SiC surface (Fig. 5a) and the volume of Si (Fig. 5b) under it is "corroded" more than in the case of growth with a high pressure of CO (Fig. 5c,d). The SiC surface represented in Fig. 5a is rough and the whole of it is covered with pyramidal bumps unlike the smoother surface of SiC represented in Fig. 5c.

Schematically the growth of SiC layer on the Si (100) and (111) surfaces covered with macro and mesopores without taking into account the type and degree of Si doping is represented in Fig. 8.

**Modeling of stress distribution.** For a qualitative assessment of the damping effect of elastic stresses in the porous SiC/Si structures and their applicability as substrates for growth of the subsequent layers of III-nitrides, a numerical simulation was conducted by the finite element method in Comsol MultiPhysics program package. During the simulation, the influence of pores on the elastic stresses arising in films with different thermal expansion coefficients at cooling and heating was studied. A numerical simulation of a 3-D substrate of centimeter size containing millions of nanometer elements seems to be a nontrivial and long task. That is why for a qualitative understanding of the processes of stress relief, a scaled two dimensional models of a film on 1mm long substrate with the porous buffer layer (Fig. 9a) as well as a film on a substrate without a buffer layer (Fig. 9b) were used. The thickness of a substrate was 0.12 mm and the thickness of the grown film was equal to 0.01 mm. The thickness of the porous buffer layer  $h$  and the period of arrangement  $p$  of the pores varied for the purpose of studying the dependence of elastic stresses on the structure of the buffer layer.

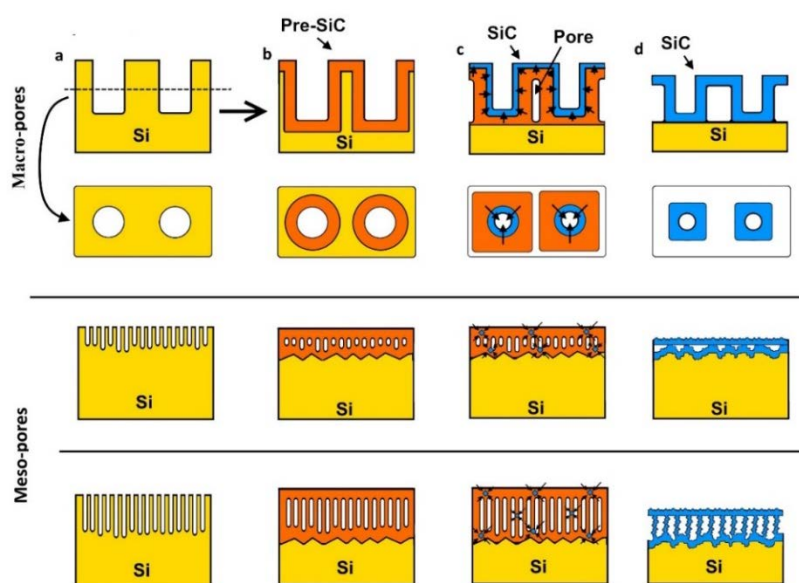


**Fig. 8.** The mechanism of formation of a SiC structure on the surface of micro and mesoporous silicon.

The thermal expansion coefficients  $\alpha$  and Young moduli  $E$  of the materials of the substrate, buffer layer, and film were chosen corresponding to Si ( $E=170$  GPa,  $\alpha=2.6 \cdot 10^{-6}$  K<sup>-1</sup> [23]), 3C-SiC ( $E=450$  GPa,  $\alpha=3.8 \cdot 10^{-6}$  K<sup>-1</sup> [23]), and GaN ( $E=300$  GPa [24],  $\alpha=3.2 \cdot 10^{-6}$  K<sup>-1</sup> [25]).

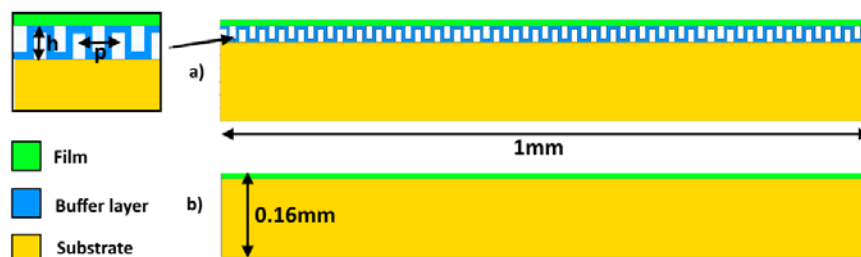


**Fig. 9.** 2-D models of structures with the porous buffer layer (a) and without it (b) used in calculations.

The thickness of walls in the buffer layer was 0.005 mm. The change of geometry of similar structures and the distribution of mechanical stresses in them during cooling from the temperature of 800 °C to room temperature at  $h=0.02$  mm and  $p=0.03$  mm are presented in Fig. 10.

In the presence of the porous buffer layer, a periodic modulation of mechanical stresses in the range of 30-103 MPa with an average value of  $\sim 65$  MPa is observed in the film. In the absence of the buffer layer, the mechanical stresses are uniformly distributed along the film surface, however, they are much higher and equal to  $\sim 125$  MPa.

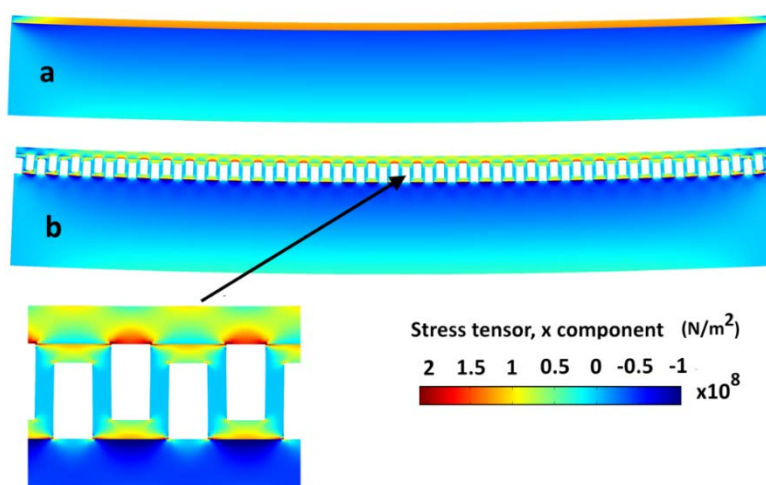


**Fig. 10.** Stress distribution in the film grown without the buffer layer (a) and with it (b) after cooling from 800 °C to room temperature.

It should be noted that in the very contact zone of the buffer layer and the film, the mechanical stresses reach the value of 140 MPa, however, they go down very quickly with the increase in film thickness. It turned out to be that increase in thickness  $h$  of the buffer layer also leads to decrease in elastic stresses. Thus, the existence of such system of pores helps to significantly reduce the mechanical stresses on a thin film surface arising owing to the differences in the TEC. It allows one to draw a conclusion about a positive influence of the system of pores on the quality of the subsequent epitaxial layers of III nitrides.

#### 4. Conclusion

The epitaxial 3C-SiC films were grown on mesoporous and macroporous Si (111) and Si (100) substrates by the method of substitution of atoms. The samples have been studied by Raman spectroscopy, scanning electron microscopy, and X-ray diffraction analysis. The studies have shown that in the case of the presence of macropores on the surface, silicon is completely converted into silicon carbide to the depth corresponding to the depth of the original pores. In the present experiment, the thickness of the resulting structure of silicon carbide is ~115 microns. In case the diameter of the initial pores exceeds hundreds of nanometers, the geometry of the SiC film after the growth process corresponds to the "skeleton" of the original porous structure, i.e. in place of the pores, hollow channels are formed, the walls of which consist of silicon carbide. The space between the channels remains empty, which is explained by a twofold decrease of the volume of the crystal cell during the transformation of Si to SiC and, as a consequence, geometrically necessary appearance of the voids. The diameter of the channels decreases after the growth process in comparison with the diameter of the initial pores by the same reason. It should be noted that in case of small sizes of the initial pores of about dozens nanometers, their original structure is not preserved. Raman and X-ray analysis show that the film consists of silicon carbide of cubic polytype, the epitaxial growth of which coincides with the (001) axis of the silicon substrate. The numerical simulation by the finite element method showed that such structures can be successfully used for the growth of subsequent layers of III-nitrides and thin films of other materials because they possess a small contact area between Si and SiC and allow to efficiently "detach" the mechanical stresses arising owing to the differences in TEC and parameters of a silicon lattice and materials of the subsequent layers.

**Acknowledgements.** S.A. Kukushkin, A.V. Osipov, A.V. Redkov and A. S. Grashchenko are grateful to the Program of Basic Research of the Presidium of the RAS «NANOSTRUCTURES: PHYSICS, CHEMISTRY, BIOLOGY, BASIS OF TECHNOLOGIES-2018» for the support of this work. S.A. Kukushkin, A.V. Osipov, V.V. Kidalov and A.F. Dyadenchuk are grateful to the Ministry for Education and Science (Russian Federation) (Grant No16.2811.2017/4.6) and the Ministry of Education and Science of Ukraine (0115U002261). I.P. Soshnikov acknowledges the Program of Russian Academy of Science «Nanostructures» for support of his part of this study.

The study was performed using equipment of the unique scientific setup «Physics, chemistry, and mechanics of crystals and thin films» of the Institute of Problems of Mechanical Engineering, Russian Academy of Sciences (St. Petersburg).

#### References

- [1] S.A. Kukushkin, A.V. Osipov, V.N. Bessolov, B.K. Medvedev, V.K. Nevolin, K.A. Tsarik // *Reviews on Advanced Materials Science* **16** (2008) 1.
- [2] S.A. Kukushkin, A.V. Osipov // *Journal of Physics D: Applied Physics* **47** (2014) 313001.
- [3] S.A. Kukushkin, A.V. Osipov, N.A. Feoktistov // *Physics of the Solid State* **56** (2014) 1507.
- [4] S.A. Kukushkin, A.V. Osipov // *Physics of the Solid State* **50** (2008) 1238.
- [5] S.A. Kukushkin, A.V. Osipov // *Journal of Applied Physics* **113** (2013) 024909.
- [6] S.A. Kukushkin, A.V. Osipov // *Physica B: Condensed Matter* **512** (2017) 26.
- [7] S.A. Kukushkin, A.V. Osipov // *Journal of Physics D: Applied Physics* **50** (2017) 464006.
- [9] S.A. Kukushkin, K.Kh. Nussupov, A.V. Osipov, N.B. Beisenkhanov, D.I. Bakranova // *Superlattices and Microstructures* **111** (2017) 899.
- [10] S.A. Kukushkin, A.V. Osipov // *Physics of the Solid State* **58** (2016) 747.

- [11] V.N. Bessolov, Yu.V. Zhilyaev, E.V. Konenkova, L.M. Sorokin, N.A. Feoktistov, Sh. Sharofidinov, M.P. Shcheglov, S.A. Kukushkin, L.I. Mets, A.V. Osipov // *Technical Physics Letters* **36** (2010) 496.
- [12] L.M. Sorokin, A.E. Kalmykov, V.N. Bessolov, N.A. Feoktistov, A.V. Osipov, S.A. Kukushkin, N.V. Veselov // *Technical Physics Letters* **37** (2011) 326.
- [13] V.V. Antipov, S.A. Kukushkin, A.V. Osipov // *Physics of the Solid State* **59** (2017) 399.
- [14] R.R. Reznik, K.P. Kotlyar, I.V. Il'kiv, I.P. Soshnikov, S.A. Kukushkin, A.V. Osipov, E.V. Nikitina, G.E. Cirilin // *Physics of the Solid State* **58** (2016) 1952.
- [15] M.M. Rozhavskaya, S.A. Kukushkin, A.V. Osipov, A.V. Myasoedov, S.I. Troshkov, L.M. Sorokin, P.N. Brunkov, A.V. Baklanov, R.S. Telyatnik, R.R. Juluri, K.B. Pedersen, V.N. Popok // *Physica Status Solidi A* **214** (2017) 1700190.
- [16] V.V. Kidalov, G.A. Sukach, A.O. Petukhov, A.S. Revenko, E.P. Potapenko // *Journal of Luminescence* **103** (2003) 712.
- [17] V.V. Kidalov, G.A. Sukach, A.S. Revenko, E.P. Potapenko // *Semiconductors* **37** (2003) 1303.
- [18] S.L. Khrypko, V.V. Kidalov // *Journal of Nano- and Electronic Physics* **8** (2016) 04071.
- [19] V.N. Bessolov, D.V. Karpov, E.V. Konenkova, A.A. Lipovskii, A.V. Osipov, A.V. Redkov, I.P. Soshnikov, S.A. Kukushkin // *Thin Solid Films* **606** (2016) 74.
- [20] S.A. Kukushkin, A.V. Osipov, A.V. Red'kov // *Semiconductors* **51** (2017) 396.
- [21] A.I. Gusev, *Nanomaterials, nanostructures, nanotechnologies* (Fizmatlit, Moscow, 2005).
- [22] S.A. Kukushkin, A.V. Osipov, I.P. Soshnikov // *Reviews on Advanced Materials Science* **51** (2017) 29.
- [23] E.L. Kern, D.W. Hamill, H.W. Deem, H.D. Sheets // *Materials Research Bulletin* **4** (1969) 25.
- [24] R.S. Telyatnik, A.V. Osipov, S.A. Kukushkin // *Physics of the Solid State* **57** (2015) 162.
- [25] M. Leszczynski, T. Suski, P. Perlin, H. Teisseyre, I. Grzegory, M. Bockowski, J. Jun, S. Porowski, J. Major // *Journal of Physics D: Applied Physics* **28** (1995) A149.